

New Challenge of Nuclear Medicine in Oncology

–The dawn of functional imaging–

Nihon Medi-Physics Co., Ltd.
Corporate Planning and Coordination Office
Strategic Marketing
Hideshi HATTORI
Research and Development Division
Research Center
Jun TOYOHARA

Today, imaging diagnosis in oncology is based on the regional anatomical information. However, anatomy-based imaging provides limited functional information and can only differentiate tumors from normal tissue based on shape, density, vascularity, fat and water. Imaging of regional tumor biology by nuclear medicine provides quantitative estimates of regional biochemistry and receptor status and can overcome the sampling error and difficulty in performing serial studies inherent with biopsy. In this review, current status of the functional imaging of tumor by nuclear medicine will be described.

This paper is translated from R&D Report, "SUMITOMO KAGAKU", vol. 2004-II.

Introduction

In many countries within Europe and North America, as well as in Japan, although there has been a gradual decrease in the number of people dying of brain and heart diseases, the number of deaths from malignant neoplasms (referred to as cancer from this point forward) has been increasing. During the year 2000, there were 295,399 cancer-related deaths in Japan, representing a mortality rate of 235.2 deaths per 100,000

people, meaning that 1 out of every 3 deaths were due to cancer¹⁾. According to the "Study on Accuracy Improvement and Usage of Local Cancer Registries"²⁾ (Research Leader: Hideaki Tsuguma) conducted by the Ministry of Health, Labour and Welfare, a breakdown of the number of cancer patients predicted in the year 2020, was as follows: 500,000 males and 350,000 females, for a total of 850,000 patients. When the number of cancer patients predicted in 2020 is compared to the number of actual cases in 2000, the annual rate of

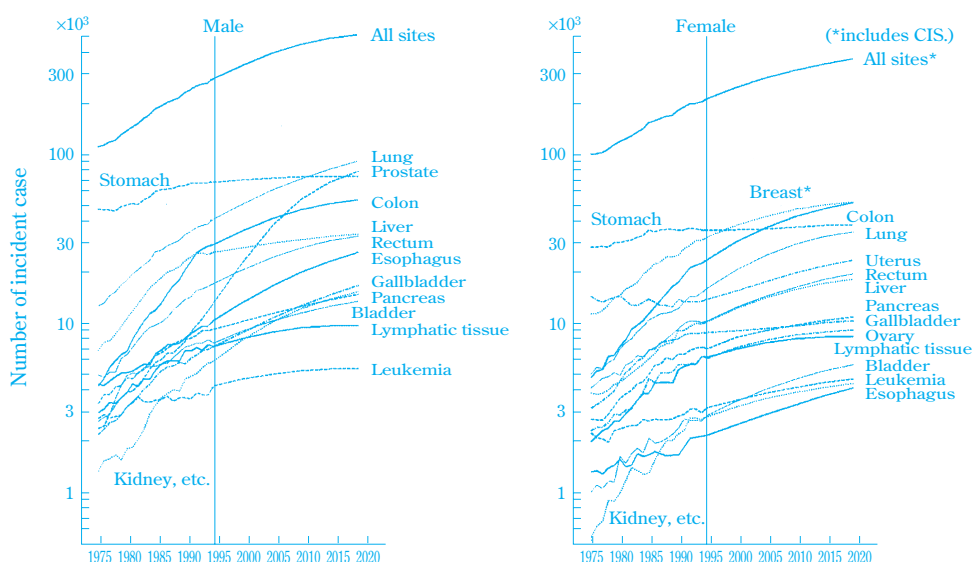


Fig. 1 Prediction of incident cases according to primary site, Japan (Data from reference¹⁾)

increase is as follows: males, 1.51; females, 1.47; for an average annual rate of increase of 1.49. These figures indicate that the number of cancer patients is expected to continue rising. **Fig. 1** depicts the prediction of incident cases according to primary site.

For males, although the number of incident cases has increased for the areas of the prostate, lung, colon, esophagus and rectum, the incidences of cancer of the stomach and liver have remained unchanged for 1995 and subsequent years. Therefore, in 2020, the number of incident cases in the lung, prostate and stomach areas are expected to remain almost exactly the same. For females, increases are seen for the areas of the colon, breast, lung, uterus, rectum and liver. However, as with males, the number of incident cases of stomach cancer has remained unchanged for 1995 and subsequent years. In the future, the number of incident cases of breast cancer is therefore predicted to exceed that of stomach cancer.

Current Status of Tumor Image Diagnosis

The relationship between trends in cancer diagnosis / treatment and diagnostic imaging varies according to the particular type of cancer and its primary site. In this section, **Table 1** depicts basic the role of diagnostic imaging throughout the various stages of cancer diagnosis and treatment.

The role of diagnostic imaging can be categorized based upon the technical characteristics of each area of application: X-ray imaging (including computed radiography: CR; and digital subtraction angiography: DSA), X-ray computed tomography (CT), magnetic resonance imaging (MRI), ultrasound (US) and nuclear medicine

(NM). In particular, the function of diagnostic imaging in the area of nuclear medicine can be classified into three modalities:

- 1) Localization diagnosis: detection of the tumor location (primary, recurrent, metastatic)
- 2) Identification diagnosis: differentiating between malignant and benign lesions, evaluation of the degree of malignancy, determination of treatment regimen
- 3) Evaluation of treatment effectiveness and response (follow-up): confirmation of tumor regression / disappearance, probability of recurrence (micro-metastasis)

Localization Diagnosis

Since localization diagnosis essentially requires high definition imaging, the role of nuclear medicine is naturally limited, as it is only able to provide images of low definition. At this present stage, nuclear medicine is useful in indicating which particular areas should be further investigated using other testing methods, in other words, for screening of the entire body. So far, the most commonly utilized NM procedures are ^{99m}Tc -Bone imaging, which is used to detect bone metastasis and ^{67}Ga imaging, which is used to perform tumor localization diagnosis. In addition, another method of localization diagnosis that employs positron emission tomography (PET), has gradually gained popularity in the field of clinical medicine. Thus, it is expected that the role of nuclear medicine will continue to expand further, in the future.

Identification Diagnosis

Subsequent to the confirmation of the location and

Table 1 Role of image diagnosis on patient management of cancer

Phase	Examination/Treatment	Image diagnosis	Role of image diagnosis
Medical checkup Outpatient	Physical examination (by interview)	X-ray	Detection of abnormal sites
		X-ray, US, CT, MRI	Identification of anatomy of abnormal sites
Precise examination	Image diagnosis Physical examination (Biopsy, etc.)	NM	Detection of distant metastasis
		MRI, NM	Differentiation diagnosis
Under treatment	Physical examination Image diagnosis	—	Determination diagnosis
		CT, MRI NM	Assessment of therapy response (Anatomy-based) Assessment of therapy response (Tumor viability)
Follow-up	Physical examination Image diagnosis	—	—
		X-ray, CT, NM	Detection of metastasis and/or recurrence

Abbreviations: US; ultrasound echo, CT; X-ray computed tomography, MRI; magnetic resonance imaging, NM; nuclear medicine.

spread of lesions using CT or MRI, the following procedures are undertaken: differentiation between malignant and benign lesions, determination of cell types, malignancy diagnosis and specification of the treatment regimen. The first choice for diagnostic action is usually a pathological diagnosis conducted on a biopsy tissue sample. However, due to the high degree of heterogeneity found within tumor tissue (tumor cells having very different characteristics and are distributed unevenly throughout a single tumor mass), the results of the pathological diagnosis can be affected by the location of the biopsy sample. Therefore, the accuracy of this type of diagnosis is considered to be only about 80%. In the event that a tissue sample cannot be obtained via biopsy, non-invasive diagnostic imaging is another possible diagnostic choice. In this case, the type of identification required, in terms of clinical medicine, consists of differentiating between malignant and benign lesions, performing a malignancy diagnosis and specifying the treatment regimen.

◆ Differentiation Between Malignant and Benign Lesions ; and Malignancy Diagnosis

Since high-resolution imaging is generally required to correctly differentiate between malignant and benign lesions, enhanced -CT (or enhanced MRI) is usually utilized. However, the accuracy of diagnosis is limited when CT or MRI techniques are utilized, as it is often difficult to determine whether any lymphadenopathy found by CT is actually due to metastasis or lymphadenitis. As this limitation is noted most frequently for cancers in the thoracic and abdominal areas, it still makes sense to utilize nuclear medicine for the diagnosis of cancers within these locations. However, the only truly practical method of identification at the present time is through ^{67}Ga imaging, which is used to identify lymphomas. Thus, nuclear medicine has not yet entered the stage in which its utility has been fully proven. Nuclear medicine-based examinations do possess the potential to replace CT and MRI, once the resolution has been improved for single photon emission computed tomography (SPECT) and PET, and after suitable second-generation tumor-specialized agents have been developed.

Furthermore, since malignancy diagnosis is a type of diagnosis that is one step beyond localization diagnosis, which is merely the anatomical diagnosis of tumors, malignancy diagnosis is now in great demand, not only in the area of diagnostic imaging, but also in

all other areas of diagnostic technology. The only method of diagnostic imaging that can presently respond to this demand is ^{18}F -FDG-PET imaging. Other existing methodologies (including enhanced CT / CT, enhanced MRI / MRI, monoclonal antibodies / SPECT) have not yet reached a satisfactory level of utility due to their own particular shortcomings.

◆ Determination of Treatment Regimen

Chemotherapy is generally performed in the event that surgical treatment is not applicable. Conventional anti-cancer drugs almost always cause side effects, as they target the difference in proliferation rates between cancer cells and normal cells. However, accompanying advances in molecular biology, specific molecules have been identified that are associated with the invasion, proliferation, vascularization and metastasis of cancer cells. Anti-cancer drugs that target these molecules (molecularly-targeted anti-cancer agents) have now been developed and put into clinical usage. It is important to carefully choose patients for whom these drugs are expected to have the most beneficial effects. It is crucial to diagnosis the patient in terms of the degree of expression of the target molecules, prior to the administration of such drugs. For example, it is now commonly known that dual HER-2 / EGFR tyrosine kinase inhibitors can be quite effective for treating cancer patients who are experiencing overexpression of target molecules.

In addition to chemotherapy, radiation therapy (or radiotherapy), is another useful treatment for cancer. It is known that cancer cells gradually become starved for oxygen (hypoxia) as the cancer progresses, thus causing a corresponding decrease in their sensitivity to radiation and thus reducing the effectiveness of radiotherapy. On the other hand, if a large dose of radiation is provided, undesirable side effects may occur, such as the bone marrow toxicity. Drugs that may help to combat these problems (radiosensitizers) are currently under development. In the future, it will become increasingly important to gain a more precise knowledge of the locations and conditions associated with cancer cell hypoxia.

Evaluating the Effects of Treatment

In principle, the first choice for tumor treatment is surgical removal. Cancer treatment is usually conducted using a combination of surgical removal, radiothera-

py and the administration of anti-cancer drugs. The effects of cancer treatment are evaluated using a variety of standards, such as improvement in the patient's overall condition, recovery of specific functions, verification of remission / disappearance of tumors and the disappearance of tumor markers within the patient's blood. The verification of tumor remission / disappearance is a process that must always be conducted subsequent to the implementation of surgical removal. Diagnostic imaging is utilized to facilitate this process. In general, since high-resolution images are required for proper verification of tumor remission, either CT or MRI are utilized and nuclear medicine examination is not usually the first choice.

However, CT and MRI do not provide any information with respect to the presence of any tumor cells within a tumor mass (= focus of necrosis or scarred connective tissue) that may still remain after treatment. In addition, as morphological changes are non-specific and occur subsequent to a functional change, a certain amount of time is required in order to evaluate the effectiveness of the treatment. Since the treatment itself is continued until its effectiveness has been evaluated, an ineffective treatment may result in economic hardship for the patient, lost opportunity to administer an alternate treatment, as well as a decrease in quality of life due to the continued administration of ineffective drugs. Thus, it is anticipated that the early stage detection of functional changes (= functional imaging) will solve these problems. As described above, although diagnostic imaging of tumor areas is conducted based on morphological information, its limitations have also been pointed out. The use of functional imaging to image the metabolic characteristics of a tumor locus is

a process that can be used to solve essential problems associated with biopsies. Nuclear medicine diagnostics has the potential to solve these problems. This paper introduces the current status of ongoing radiopharmaceutical research conducted for the purpose of facilitating effective functional imaging.

Current Status of Radiopharmaceutical Research in the Field of Oncology

Table 2 lists certain radiopharmaceuticals that are utilized for the functional imaging of tumor biology. **Fig. 2** depicts the chemical structures of various positron-labeled radiopharmaceuticals.

1. Imaging of Glucose Metabolism

In a malignant tissue, the proliferation of neoplastic cells usually progresses at a greater rate than the corresponding tissue vascularization, thus producing a hypoxic tissue fraction. As tumor cells continue to multiply within this hypoxic environment, they are forced

Table 2 Radiopharmaceuticals for functional imaging of tumor biology

Biological/biochemical function	Radiopharmaceutical
Glucose metabolism	^{18}F -FDG
Amino acid transport and incorporation	^{18}F -FACBC
Membrane/lipid biosynthesis	^{11}C -acetate, ^{11}C -choline, ^{18}F -FCH
DNA synthesis	^{18}F -FLT
Hypoxia	^{18}F -fluoromisonidazole, ^{62}Cu -ATSM
Apoptosis	$^{99\text{m}}\text{Tc}$ -AnnexinV
Receptor expression	^{18}F -FES, ^{123}I -MIBG, ^{111}In -DTPA-octreotide
P-glycoprotein	$^{99\text{m}}\text{Tc}$ -MIBI, $^{99\text{m}}\text{Tc}$ -tetrofosmine

See text for definition of abbreviations

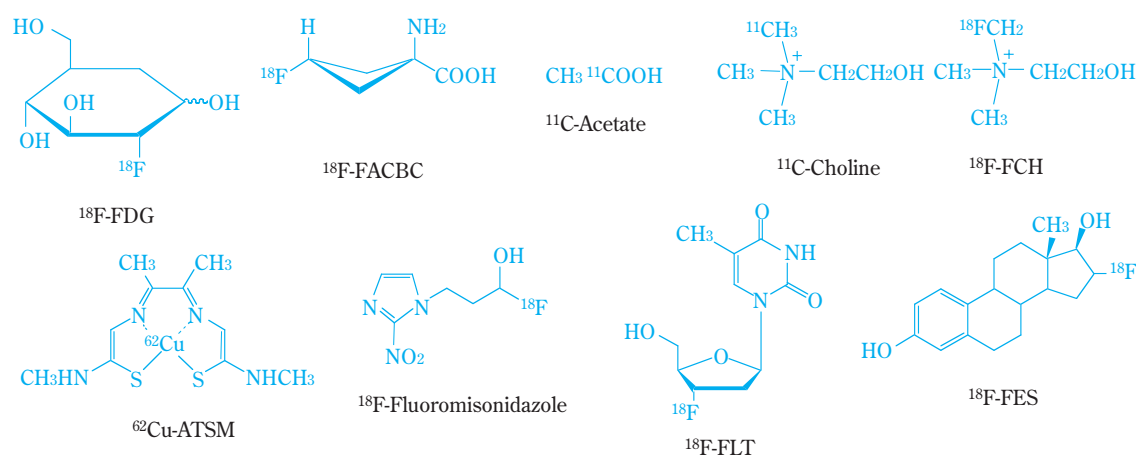


Fig. 2 Chemical structures of positron labeled radiopharmaceutical for tumor functional imaging

to obtain energy by taking advantage of the anaerobic glycolysis of glucose.³⁾ For this reason, an increase in glucose transporters and hexokinase activity can be recognized in tumor cells. These increases demonstrate a characteristic increase in the ability of tumor cells to uptake large quantities of glucose.⁴⁾ Furthermore, tumor cells also have a lower incidence of glucose-6-phosphatase activity (phosphatase of glucose-6-phosphoric acid).⁴⁾ The radiopharmaceutical known as 2-deoxy-2-[¹⁸F] fluoro-D-glucose (¹⁸F-FDG) (Fig. 2), in which the secondary hydroxyl group has been replaced with ¹⁸F, accumulates rapidly in a variety of different tumor types. Since April 1 of 2002, ¹⁸F-FDG, which can be used to diagnose lung cancer, breast cancer, colon cancer, head and neck cancer, brain tumors, pancreatic cancer, malignant lymphoma, metastatic liver cancer, non-site-specific cancers and malignant melanoma, with these patients also fulfill given specific requirements, have been utilized in a number of applications involving medical examinations. In general, since ¹⁸F-FDG is more readily taken up by tumors having a high degree of malignancy, it is often utilized in the following areas: identification diagnosis; staging diagnosis; and in diagnosis for metastasis and recurrence. In addition, as the rate of tissue accumulation of ¹⁸F-FDG is proportional to the number of cells that are active in glucose metabolism (= living cells)⁵⁾, ¹⁸F-FDG has been utilized in quantitative evaluations of the effects of both chemotherapy and radiotherapy. Wieder et al., had conducted testing with positron emission tomography ¹⁸F-FDG (¹⁸F-FDG-PET) on 38 cancer patients (cT3, cN0/+, cM0) with esophageal squamous cell carcinoma (whose esophagectomies were scheduled after preoperative chemoradiation therapy had been conducted for a period of 4 weeks) prior to their preoperative chemoradiation therapy and subsequent operations. The changes observed in glucose metabolism were then compared to response evaluation criteria according to histopathological response.⁶⁾ The following results were obtained from this comparison testing: in histopathologically responding cases, ¹⁸F-FDG-PET studies indicated that glucose metabolism had decreased by 70±11%. In histopathologically non-responding cases, glucose metabolism was seen to have decreased by 51±21%. In ¹⁸F-FDG-PET studies conducted on the 14th day after the initiation of preoperative treatment, tumor glucose metabolism changes in histopathologically responding cases were detected at a sensitivity of 93% and a specificity of

88%. Furthermore, such changes correlated significantly with patient survival time ($p = 0.011$). **Fig. 3** depicts examples of images obtained from ¹⁸F-FDG-PET studies (coronal slices). The upper images (A) depict the histopathologically responding tumors, with the lower images (B) depicting non-responding tumors. In the histopathologically responding tumors, a significant decrease was observed in the accumulation of ¹⁸F-FDG after the 14th day of continued preoperative chemoradiation therapy. However, no corresponding decrease in ¹⁸F-FDG accumulation was recognized in the non-responding tumors. According to the treatment response evaluation of chemotherapy, the utility of ¹⁸F-FDG has been proven for use in the diagnosis of stomach cancer and breast cancer.^{7, 8)}

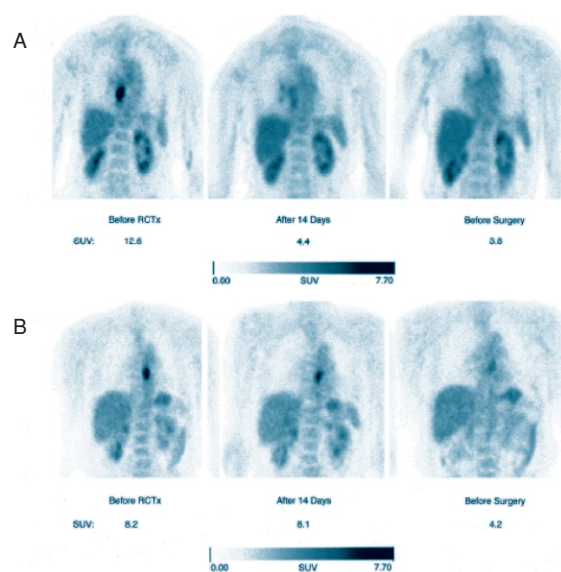


Fig. 3 Example of ¹⁸F-FDG-PET studies (coronal slices) in (A) histopathologically responding and (B) nonresponding tumors. RCTx, chemotherapy; SUV, standardized uptake value. (Data from reference⁶⁾).

Glucose metabolism comparison tests were conducted during chemotherapy treatment of a progressive cancer, as follows: ¹⁸F-FDG-PET examinations were conducted on 57 patients with progressive non-small cell lung cancer (stage IIIb or IV), both prior to the administration of cisplatin-based chemotherapy and after the administration of a single treatment cycle. Changes in tumor glucose metabolism were then compared to Response Evaluation Criteria in Solid Tumors (RECIST)⁹⁾ during the follow-up process.¹⁰⁾ As a result of this comparison, the changes in tumor glucose metabolism were considered to be predictable indica-

tors for response evaluation criteria ($p < 0.0001$: sensitivity of 95%; specificity of 74%). As well, changes in the tumor glucose metabolism observed using ^{18}F -FDG correlated well with both median time to progression, as well as with overall survival (median time to progression: $p = 0.0003$; overall survival: $p = 0.005$).

The following conclusions can be derived from the above findings: tumor glucose metabolism comparisons conducted using ^{18}F -FDG-PET can be used for early stage identification of tumors that do not respond to preoperative chemoradiation therapy, thus enabling physicians to make earlier revisions to the treatment protocol. In addition, the consideration of ^{18}F -FDG-PET tumor glucose metabolism imaging as an endpoint can shorten the evaluation period for the treatment regimen, resulting in improved survival rates and reductions in overall treatment costs.

2. Imaging of Amino Acid Transport / Uptake

^{18}F -FDG accumulates in normal tissues that have high levels of glucose metabolism, such as brain, as well as at sites of inflammation during the acute stage, which is marked by the accumulation of various inflammatory cells. These factors render ^{18}F -FDG imaging difficult in applications for the diagnosis of brain tumors and other diagnoses that must be conducted immediately after treatment. On the other hand, protein synthesis in the brain is not as active as that occurring within other organs, such as the pancreas and the liver. This fact is now attracting attention as a metabolic function that can be used in the positive diagnostic imaging of brain tumors. Since amino acids comprise the fundamental building blocks for protein synthesis and since malignant tumors require a high rate of amino acid uptake for cell proliferation, it can be concluded that ^{18}F -labeled amino acid derivatives will gain widespread utilization as tumor diagnosis agents in PET applications, supplementing the use of ^{18}F -FDG.

Recently, Shoup et al., synthesized a compound known as 1-amino-3- ^{18}F fluorocyclobutane-1-carboxylic acid (^{18}F -FACBC) (Fig.2), which is an ^{18}F -labeled version of a non-natural, biologically stable, amino acid called α -aminocyclobutane carboxylic acid (ACBC). The researchers were subsequently able to demonstrate the compound's clinical utility in diagnostic imaging.¹¹⁾ It is presumed that the mechanism of ^{18}F -FACBC accumulation within cells is via amino acid transport carriers that are present on the surface of the cell membrane. However, the details behind the func-

tioning of this mechanism have not yet been identified. **Fig. 4** depicts images from clinical research conducted using ^{18}F -FACBC. In the gadolinium-enhanced MRI / T1 images (trans-axial cranium section) of a patient with neuronal glioblastoma taken prior to surgical tumor removal, it is observed that the tumor in the left frontal lobe has spread to the opposite lobe (top row images). While the ^{18}F -FACBC-PET imaging (bottom row images) performed one week after the operation indicates an abnormal accumulation of ^{18}F -FACBC, the ^{18}F -FDG-PET imaging (middle row images) performed 8 weeks after the operation indicates no such abnormal accumulation. In a subsequent operation, it was confirmed that the area in which abnormal accumulation of ^{18}F -FACBC was seen, contained the remaining neural glioblastoma. These results therefore suggest that ^{18}F -FACBC-PET imaging can be effective in the diagnosis of brain tumors, in the following ways: tumor diagnosis; location diagnosis; evaluation of degree of malignancy; effects of treatment and determination of recurrence.

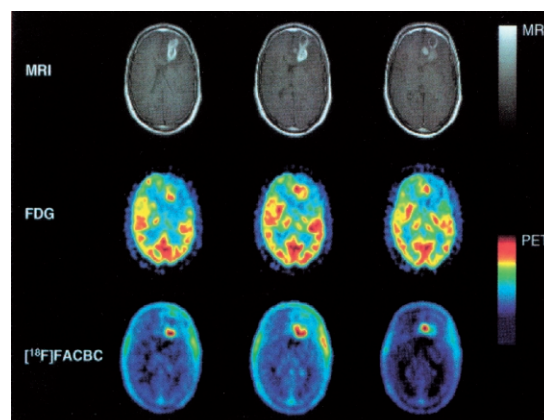


Fig. 4 ^{18}F -FACBC-PET images of patient with glioblastoma multiform (bottom row). Top row: T1-weighted transaxial MRI scans with gadolinium enhancement. Middle row: ^{18}F -FDG-PET images. (Data from reference¹¹⁾).

3. Imaging of Membrane Biosynthesis / Lipogenesis

In order to support cell proliferation, which is one of the primary characteristics of malignant tumors, membrane and lipid (both of which are components of cell membranes) biosyntheses is also required, in addition to DNA synthesis. Therefore, radiopharmaceuticals that target the biosyntheses of membranes and lipids have the potential to become new functional diagnostic agents for tumors.

[1-¹¹C]-Acetate (Fig. 2) is a radiopharmaceutical that has been developed for the purpose of evaluating the aerobic metabolism of the TCA cycle in cardiac muscle. However, it is known that the acetyl-CoA produced during acetate metabolism is used not only for aerobic energy production, but also for the biosynthesis of lipids, such as phospholipids.^{12, 13)} Yoshimoto et al., therefore hypothesized that within malignant tumor cells having a high degree of proliferation, acetate metabolism has actually shifted to lipogenesis, since energy metabolism in the tumor depends greatly upon the aerobic energy produced via the glycolytic pathway. Based on this hypothesis, the researchers conducted a fundamental examination into the relationship between acetate metabolism within the tumor and the degree of tumor cell proliferation.¹⁴⁾ The results indicated that the [1-¹⁴C]-acetate taken into tumor cells was a component of lipophilic metabolites (phosphatidyl choline and glyceride), as had been predicted. In addition, the quantity of radioactivity absorbed by the [1-¹⁴C]-acetate in the lipophilic fraction showed a strong correlation with the amount of [methyl-³H]thymidine (used as an index of cell proliferation) incorporated into the DNA ($p = 0.0016$).

Unlike ¹⁸F-FDG, [1-¹¹C]-acetate releases only a minimal amount of radioactivity into urine, which has made it useful in clinical studies for both the detection and disease stage diagnosis of pelvic neoplasms adjacent to the bladder, particularly prostate cancer. **Fig. 5** depicts the clinical images of the ¹¹C-acetate in a patient with poorly differentiated adenocarcinoma of

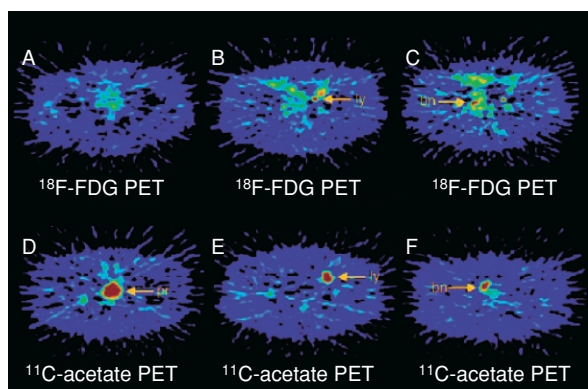


Fig. 5 PET images of prostate, lymph node, and bone metastases obtained using ¹⁸F-FDG (upper row) and ¹¹C-acetate (bottom row) from 73-y-old man with poorly differentiated (Gleason score 7) adenocarcinoma of prostate. bn=bone; ly=lymph node; pr=prostate. (Data from reference¹⁵⁾).

prostate.¹⁵⁾ In the ¹⁸F-FDG-PET images shown in the upper row, no abnormalities were detected, as the level of ¹⁸F-FDG accumulation in the primary lesion (A), was low. The ¹⁸F-FDG-PET images did indicate lymph node metastasis to the left ilium (B) and bone metastasis to the right pubic bone. The ¹¹C-Acetate-PET images shown in the bottom row clearly indicate the primary lesion (D), left ilium lymph node metastasis (E) and bone metastasis to the right pubic bone (F).

Furthermore, an acceleration of choline metabolism has been confirmed in malignant tumors, corresponding to the acceleration of cell membrane phosphatide biosynthesis. The dynamics of choline metabolism within tumor tissue have been increasingly clarified through numerous studies involving MR spectroscopy and biochemical research. Therefore, in tumor cells that are undergoing vigorous cell division, there is an acceleration of choline kinase activity, which causes increased concentrations of choline, phosphocholine and phosphoethanolamine within the cell. It has been speculated that after uptake by the cell, the choline undergoes phosphorylation by choline kinase and then remains within the tumor tissue.

Hara et al., in studies employing ¹¹C-choline (Fig. 2), reported that certain choline derivatives can be employed as imaging agents for brain tumors and prostate cancer.^{16, 17)} Furthermore, DeGrado et al., have developed a very useful compound known as [¹⁸F]fluoromethyl-dimethyl-2-hydroxyethyl-ammonium (¹⁸F-FCH) (Fig. 2).¹⁸⁾ As with [1-¹¹C]-acetate, ¹¹C-choline does not release much radioactivity into the urine, thus it is expected to find application in prostate cancer diagnosis. ¹⁸F-FCH was found to have limited utility in applications for prostate cancer diagnosis, as unlike ¹¹C-choline, it releases radioactivity into the urine immediately.

4. Imaging of DNA Synthesis

Research into the imaging of DNA synthesis using nucleic acid derivatives is being conducted in order to evaluate the effectiveness of chemotherapy and radiotherapy treatments for malignant tumors. The use of ¹¹C-thymidine has been studied, based on a method of evaluating DNA synthesis that utilizes [methyl-³H]thymidine as a cell proliferation marker. However, certain problems, including excess noise due to the short physical half-life of the ¹¹C (approximately 20 minutes) and the secondary distribution of ¹¹C-labeled metabolites, made it difficult to conduct a quantitative

evaluation of tumor proliferation from the images obtained. In order to solve these problems, Shields and researchers attempted to use ^{18}F -labeled 3'-deoxy-3'-fluorothymidine (FLT), which was originally developed as an anti-viral agent, resulting in the successful synthesis of ^{18}F -FLT (Fig. 2).¹⁹⁾ Fig. 6 depicts the first clinical case in which ^{18}F -FLT was administered to a patient with non-small cell lung cancer. Fig. 6 shows a coronal image on the left, a sagittal image on the right and transverse scans in the middle. ^{18}F -FLT accumulation can be observed in the following locations: tumors having high degree of proliferation, bone marrow, the liver and the bladder; the latter two organs functioning in metabolism / excretion. The accumulation of ^{18}F -FDG was also observed in the tumor, however, no corresponding accumulation of radioactivity due to ^{18}F -FDG was observed in the bone marrow.

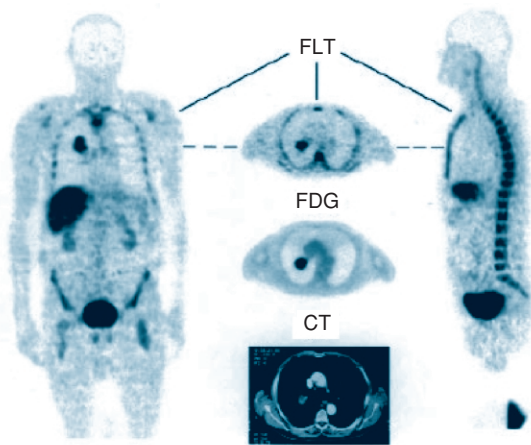


Fig. 6 ^{18}F -FLT images of patient with non-small cell lung cancer. Left: coronal image. Right: sagittal image. Center: transverse image. (Data from reference¹⁸⁾).

^{18}F -FLT is incorporated into DNA synthesis pathways subsequent to the phosphorylation of the 5'-hydroxyl group. However, as the 3'-hydroxyl group has been replaced with fluorine, no phosphodiester bond is formed, thus preventing the replication of the DNA chain. On the other hand, the ^{18}F -FLT accumulated after phosphorylation cannot easily be dispersed outside of the cell due to its negative charge, thus it remains within the cell. The intracellular level of ^{18}F -FLT accumulation therefore reflects the thymidine kinase (TK1) activity, thus providing imaging that expresses an indirect indication of the level of DNA synthesis.

Toyohara et al., utilized 22 tumor cell lines, each possessing a different degree of proliferation, in a study to determine whether the intercellular accumulation of FLT that reflects TK1 activity would also reflect the degree of cell proliferation.²⁰⁾ The results of this study demonstrated that cellular FLT uptake is strongly correlated with the uptake of [methyl- ^3H]thymidine and the %S-phase, cell proliferation markers. In addition, Rasey et al., used non-small cell lung cancer cell lines having synchronized cell cycles, to study whether the accumulation of FLT is dependent upon cell cycle. They were able to confirm that the pattern of FLT uptake indicates that FLT accumulation is dependent upon cell cycle.¹⁹⁾ Furthermore, an examination of the histopathology showed that there was a strong correlation ($r = 0.87$; $p < 0.0001$) between the accumulated ^{18}F -FLT radioactivity levels in solitary human pulmonary nodules and the degree of staining in the cell proliferation marker Ki-67 (Fig. 7).²²⁾

These findings are the result of proactive support for the hypothesis that the proliferation dynamics of malignant tumor cells can be imaged non-invasively, using ^{18}F -FLT. However, the following phenomenon has also been reported: the level of ^{18}F -FLT accumulation in each cell increases in the presence of either the de novo synthesis inhibitor 5-fluorouracil (5-FU), as well as methotrexate (MTX), thus causing discrepancy between ^{18}F -FLT accumulation and cell proliferation dynamics.²³⁾ This phenomenon is derived from the fact that the level of ^{18}F -FLT accumulation in each cell increases as TK1 (a salvage pathway enzyme) activity accelerates, due to enzymatic inhibition of de novo syn-

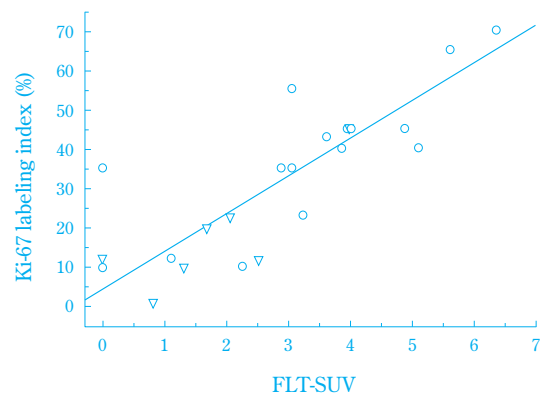


Fig. 7 Linear regression analysis demonstrated a significant correlation between proliferative fraction and ^{18}F -FLT uptake in solitary pulmonary nodule. (Data from reference²²⁾).

thesis. Therefore, further testing is needed before ^{18}F -FLT can be properly used in the evaluation of anti-tumor drug effectiveness.

5. Imaging of Hypoxia

Hypoxic tissues can be defined as “tissues that are still within the range of structural normality, yet in which reversible changes are occurring due to a lack of oxygen.” In a malignant tumor, the rate of tissue vascularization is slower than that required by the vigorous proliferation of tumor cells, thus creating hypoxic regions. Since hypoxic tumors are considered to have low radiosensitivity, it is difficult to obtain satisfactory effects from radiotherapy. Therefore, it is expected that the imaging of hypoxic regions within tumors may provide information that is useful for planning dose distributions and irradiation target sites during Intensity Modulated Radiation Therapy (IMRT).

With respect to imaging agents for hypoxic tissues, ^{18}F -fluoromisonidazole (Fig. 2) has been commonly utilized. ^{18}F -Fluoromisonidazole is a derivative of a nitroimidazole compound that was developed as a radiosensitizing agent. However, as the nitroimidazole compound was originally developed as a scavenger for unstable radicals produced within the cell due to radiation exposure, numerous factors pertaining to its mechanism of accumulation are still unknown. Focusing upon the fact that copper (Cu) contributes to oxidation-reduction reactions within living organisms, Fujibayashi et al., synthesized a hypoxic tissue diagnostic agent using a $^{62}\text{Zn} / ^{62}\text{Cu}$ generator known as ^{62}Cu -diacetyl-bis (N⁴-methylthiosemicarbazone) (^{62}Cu -ATSM) (Fig. 2). The agent was labeled with ^{62}Cu , which has a positron emitting nucleus, and was subsequently utilized in the imaging of tumors.^{24, 25} The ^{62}Cu -ATSM showed a high level of accumulation in the tumor. As well, unlike ^{18}F -FDG, it also resulted in images that appeared to reflect non-uniformities in the blood flow. Furthermore, Obata et al., have determined that Cu-ATSM accumulates and remains within tumor cells due to reduction caused by the electron transfer system enzyme of microsomes that express vigorously within tumor cells.²⁶

6. Imaging of Apoptosis

Based on the fact that anti-cancer drugs induce apoptosis in cancer cells, the phenomenon of apoptosis is considered important as it directly produces the successful effects of chemotherapy. Therefore, if imaging

can be used to determine the degree of tumor cell apoptosis after anti-cancer drug administration, then this imaging may facilitate the evaluation of tumor sensitivity to such drugs, thus allowing for better prediction of treatment effectiveness.

Blankenberg et al., sought a method for detecting apoptosis in vivo. They initially synthesized $^{99\text{m}}\text{Tc}$ -HYNIC-AnnexinV, which possesses a strong affinity for PS. The phosphatidylserine (PS) expressed on the surface of cell membranes, which can be observed in the early stages of apoptosis. Blankenberg et al., subsequently used a variety of animal models to demonstrate that apoptosis can be detected in vivo using $^{99\text{m}}\text{Tc}$ -HYNIC-AnnexinV.²⁷ Furthermore, Belhocine et al., conducted phase I / II clinical testing with $^{99\text{m}}\text{Tc}$ -AnnexinV on 10 lung cancer patients, 2 breast cancer patients and 3 patients with malignant lymphomas²⁸. Throughout this testing, the changes in the accumulations of $^{99\text{m}}\text{Tc}$ -AnnexinV were examined both before and after a single course of chemotherapy. The chemotherapy proved effective in 8 cases of lung cancer and malignant lymphoma, in which $^{99\text{m}}\text{Tc}$ -AnnexinV accumulation levels had been seen to increase (= apoptosis was detected). The chemotherapy was not effective for the 5 such cases in which $^{99\text{m}}\text{Tc}$ -AnnexinV accumulation levels were not seen to increase. For the 2 cases of breast cancer, no correlation was found between changes in $^{99\text{m}}\text{Tc}$ -AnnexinV accumulation levels and the effectiveness of the chemotherapy.²⁸ These results suggest that for lung cancer and malignant lymphomas, the effectiveness of chemotherapy can be predicted using $^{99\text{m}}\text{Tc}$ -AnnexinV. **Fig. 8** depicts the images taken during phase I / II clinical testing with $^{99\text{m}}\text{Tc}$ -AnnexinV. In the non-responding case (PD) of non-small cell lung cancer (A), no accumulation of radioactivity was observed in the $^{99\text{m}}\text{Tc}$ -AnnexinV image taken after therapy (A2), as compared to the $^{99\text{m}}\text{Tc}$ -AnnexinV image taken prior to therapy (A1). In the responding case (CR) of non-small cell lung cancer (B), the $^{99\text{m}}\text{Tc}$ -AnnexinV image taken after therapy (B2) showed a greater accumulation of radioactivity in the metastasis lesions of the cervical area, as well as in the bilateral bronchopulmonary lymph nodes (areas indicated by arrows), as compared to the $^{99\text{m}}\text{Tc}$ -AnnexinV image taken prior to therapy (B1). In the responding case (CR) of non-Hodgkin's lymphoma, the $^{99\text{m}}\text{Tc}$ -AnnexinV image taken after therapy (C2) showed a greater accumulation of radioactivity in the metastasis lesions

in the cervical nodes, as well as in the left axillary nodes (areas indicated by arrows), as compared to the ^{99m}Tc -AnnexinV image taken prior to therapy (C1).

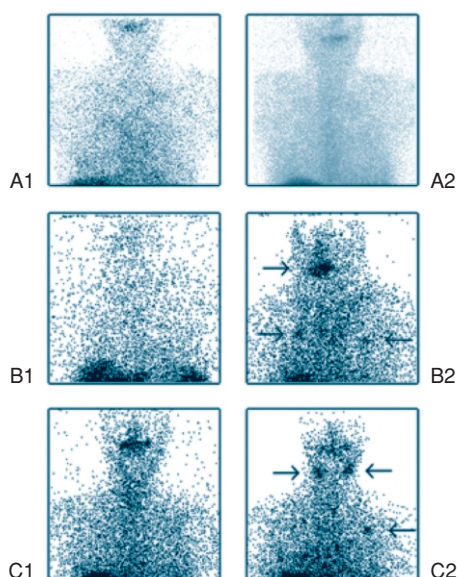


Fig. 8 Example of ^{99m}Tc -AnnexinV imaging studies in responding (B and C) and nonresponding (A) tumors. A and B: Case of non-small cell lung cancers. C: A case of non-Hodgkin's lymphoma. (Data from reference²⁸).

7. Imaging of Receptors

In certain tumors, the presence of specific cells and receptors can be observed. Therefore, the imaging of such tumors has been attempted using chemical compounds that possess an affinity for the transporters and receptors present in the subject cells.

^{123}I -m-iodobenzylguanidine (^{123}I -MIBG) is a chemical compound derived from guanethidine, which is an anti-hypertension agent that blocks sympathetic nerve action. As this compound is taken up by the adrenal medulla and sympathetic nerve endings via the same mechanism as that of norepinephrine, it has been utilized for scintigraphy of the adrenal medulla and for the diagnosis of sympathetic nerve function in cardiac muscle. The first known application of MIBG in tumor imaging was for the scintigraphy of a pheochromocytoma using ^{131}I -MIBG, as reported by Sissonn et al.²⁹ Since then, many instances of MIBG usage have been reported in the diagnoses of pheochromocytomas, as well as in regional diagnosis of neuronal glioblastomas, thyroid medullary carcinomas, carcinoids and lung cancers.

Somatostatin receptors are found in abundance with-

in neuroendocrine tumor cells, allowing radiolabeled compounds that bond to somatostatin receptors to be utilized as highly specific radiopharmaceuticals. Although somatostatin is a peptide composed of 14 amino acids, the location of receptor binding occurs at Phe7-Trp-Lys-Thr10. (D)-Phe-Cys-Phe-(D)-Trp-Lys-Thr-Cys-The(ol) (octreotide) was utilized as a precursor compound (peptidase resistance was added through conversion of some constituent amino acids into D-types) in the synthesis of ^{111}In -DTPA-octreotide, through the following process: DTPA was introduced as a chelation site to the D-Phe residue, located at the N-end. The radiolabeling of ^{111}In then occurred via this DTPA.³⁰ Octreotide demonstrates a high positive rate of binding to neuroendocrine tumors, such as hypophyseal adenomas, pancreas endocrine tumors, pheochromocytomas, neuroblastomas, paragangliomas, carcinoids, thyroid medullary carcinomas and small cell lung cancers. In particular, ^{111}In -DTPA-octreotide is extremely useful in the diagnoses of primary and metastatic lesions in pancreas endocrine tumors and carcinoids, all of which are difficult to detect using only CT or MRI.

Today, it is estimated that two-thirds of all breast cancer cases will respond to hormone treatments. It is also presumed that the degree of response can be predicted by observing the expression of estrogen receptors (ER) and progesterone receptors (PR). Therefore, in the field of breast cancer treatment, it is expected that receptor density may be predicted not only for primary lesions, but also for a broader range, such as for metastatic lesions, once it becomes possible to obtain ER and PR information through diagnosis via nuclear medicine imaging. At present, although no radiopharmaceuticals have yet proven effective in the imaging of PR, a compound known as 16α -[^{18}F]fluoroestradiol-17 β (^{18}F -FES) (Fig. 2) has been developed for the imaging of ER. A correlation has been reported between the accumulation of ^{18}F -FES and the results of in vitro receptor binding assays.^{31, 32} Fig. 9 shows coronal images taken of a breast cancer case, using ^{18}F -FDG-PET (left) and ^{18}F -FES-PET (right).³³ Positive ER expression was confirmed through a biopsy of a left axillary lymph node. Although the accumulation of ^{18}F -FES was observed in the metastatic left axillary lymph nodes, an accumulation of ^{18}F -FDG in a bone metastasis within the spine could not be observed. Although the metastatic left axillary lymph node responded to a subsequent hormone treatment, the bone metastatic

lesion became progressed. From this fact, it can be concluded that ^{18}F -FES-PET imaging is capable of detecting heterogeneous ER expression in metastasis.

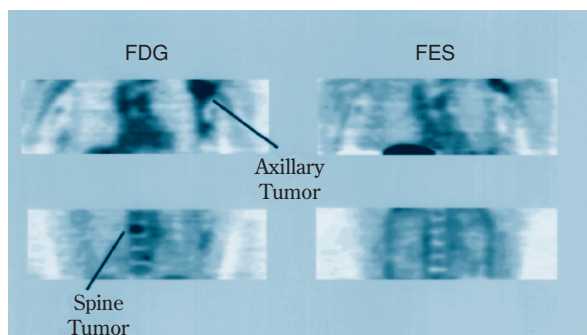


Fig. 9 Heterogeneous ER expression demonstrated by PET imaging. (Data from reference³³).

Furthermore, a correlation was reported between the accumulation characteristics of ^{18}F -FES and the action of tamoxifen, thus suggesting the possibility of ^{18}F -FES application in the prediction of treatment effectiveness.³⁴

8. Imaging of P-Glycoproteins

The compounds $^{99\text{m}}\text{Tc}$ -2-hexakis-2-methoxybutyl-isonitrile ($^{99\text{m}}\text{Tc}$ -MIBI) and $^{99\text{m}}\text{Tc}$ -1, 2-bis[bis (2-ethoxyethyl) phosphino]ethane ($^{99\text{m}}\text{Tc}$ -tetrofosmin) were developed as scintigraphy agents for use in the imaging of myocardial blood flow. Since these compounds also accumulate within certain malignant tumors, their levels of accumulation and subsequent rates of washout have drawn attention, in terms of their relationships with the multiple drug resistance possessed by certain anti-cancer drugs. Delayed imaging has demonstrated that tumors in which the above scintigraphy agents washout rapidly show the expression of P-glycoproteins, thus indicating that such tumors possess the characteristics of multiple drug resistance.^{35, 36}

Conclusion

Now that medicine has entered the 21st century, new molecular-targeted anti-cancer drugs, such as imatinib mesylate and Gefitinib have been triumphantly heralded in the treatment of malignant tumors. Currently, among pharmaceutical agents that are considered by drug manufacturers to be potential candidates

for development, there exist many molecular-targeted drugs that target gene products, which are a cause of malignant tumors. This fact suggests that future treatment regimens will more frequently be determined according to the biological characteristics of malignant tumors. We therefore expect that functional imaging of tumor metabolic functions to have tremendous potential for improving both the quality of life and the effectiveness of treatment, for cancer patients. We also believe that our company has a great responsibility to meet these needs, as a manufacturer of radiopharmaceutical products.

References

- 1) STATISTICS AND INFORMATION DEPARTMENT, MINISTER'S SECRETARIAT, MINISTRY OF HEALTH, LABOUR AND WELFARE "VITAL STATISTICS OF JAPAN"
- 2) Ohno, Y., Tsukuma, H., et al. (2004) Projection of Japanese cancer incidences based on the analyses using a Bayesian age-period-cohort model, Cancer Mortality and Morbidity Statistics.
- 3) Warburg O.: On the origin of cancer cells. *Science* **123**, 309–314 (1956).
- 4) Waki A. et al.: Recent advances in the analysis of the characteristics of tumors on FDG uptake. *Nucl Med Biol* **25**, 589–592 (1998).
- 5) Kubota R. et al.: Intratumoral distribution of fluorine-18-fluorodeoxyglucose in vivo: high accumulation in macrophages and granulation tissues studied by microautoradiography. *J Nucl Med* **33**, 1972–1980 (1992).
- 6) Wieder H.A. et al.: Time course of tumor metabolic activity during chemoradiotherapy of esophageal squamous cell carcinoma and response to treatment. *J Clin Oncol* **22**, 900–908 (2004).
- 7) Ott K. et al.: Prediction of response to preoperative chemotherapy in gastric carcinoma by metabolic imaging: Results of prospective trial. *J Clin Oncol* **21**, 4604–4610 (2003).
- 8) Smith I.C. et al.: Positron emission tomography using [^{18}F]-fluorodeoxy-D-glucose to predict the pathological response of breast cancer to primary chemotherapy. *J Clin Oncol* **18**, 1676–1688 (2000).
- 9) Therasse P. et al.: New guidelines to evaluate

- the response to treatment in solid tumors: European Organization for Research and Treatment of Cancer National Cancer Institute of the United States National Cancer Institute of Canada. *J Natl Cancer Inst* **92**, 205–216 (2000).
- 10) Wolfgang A. et al.: Positron emission tomography in non-small-cell lung cancer: prediction of response to chemotherapy by quantitative assessment of glucose use. *J Clin Oncol* **21**, 2651–2657 (2003).
 - 11) Shoup T.M. et al.: Synthesis and evaluation of [¹⁸F]1-amino-3-fluorocyclobutane-1-carboxylic acid to image brain tumors. *J Nucl Med* **40**, 331–338 (1999).
 - 12) Howard B.V.: Acetate as a carbon source for lipid synthesis in cultured cells. *Biochem Biophys Acta* **488**, 145–151 (1977).
 - 13) Long V.J.W.: Incorporation of 1-¹¹C-acetate into the lipids of isolated epidermal cells. *Br J Dermatol* **94**, 243–252 (1976).
 - 14) Yoshimoto M. et al.: Characterization of acetate metabolism in tumor cells in relation to cell proliferation: Acetate metabolism in tumor cells. *Nucl Med Biol* **28**, 117–122 (2001).
 - 15) Oyama N. et al.: ¹¹C-acetate PET imaging of prostate cancer. *J Nucl Med* **43**, 181–186 (2000).
 - 16) Hara T. et al.: PET imaging of brain tumor with [methyl-¹¹C]choline. *J Nucl Med* **38**, 842–847 (1997).
 - 17) Hara T. et al.: PET imaging of prostate cancer using carbon-11-choline. *J Nucl Med* **39**, 990–995 (1998).
 - 18) DeGrado T.R. et al.: Synthesis and evaluation of ¹⁸F-labeled choline as an oncologic tracer for positron emission tomography: initial findings in prostate cancer. *Cancer Res* **61**, 110–117 (2001).
 - 19) Shields et al.: Imaging proliferation in vivo with [¹⁸F]FLT and positron emission tomography. *Nat Med* **4**, 1334–1336 (1998).
 - 20) Toyohara et al.: Basis of FLT as a cell proliferation marker: comparative uptake studies with [³H]thymidine and [³H]arabinothymidine and cell analysis in 22 asynchronously growing tumor cell lines. *Nucl Med Biol* **29**, 281–287 (2002).
 - 21) Rasey J.S. et al.: Validation of FLT uptake as a measure of thymidine kinase-1 activity in A549 carcinoma cells. *J Nucl Med* **43**, 1210–1217 (2002).
 - 22) Buck A.K. et al.: 3-deoxy-3-[¹⁸F]fluorothymidine-positron emission tomography for non-invasive assessment of proliferation in pulmonary nodules. *Cancer Res* **62**, 3331–3334 (2002).
 - 23) Dittmann H. et al.: Early changes in [¹⁸F]FLT uptake after chemotherapy: an early experimental study. *Eur J Nucl Med Mol Imaging* **29**, 1462–1469 (2002).
 - 24) Fujibayashi Y. et al.: Copper-62-ATSM: a new hypoxia imaging agent with high membrane permeability and low redox potential. *J Nucl Med* **38**, 1155–1160 (1997).
 - 25) Takahashi N. et al.: Evaluation of ⁶²Cu labeled diacetyl-bis(*N*⁴-methylthiosemicarbazone) as a hypoxic tissue tracer in patients with lung cancer. *Ann Nucl Med* **14**, 323–328 (2000).
 - 26) Obata A. et al.: Retention mechanism of hypoxia selective nuclear imaging/radiotherapeutic agent Cu-diacetyl-bis(*N*⁴-methylthiosemicarbazone) (Cu-ATSM) in tumor cells. *Ann Nucl Med* **15**, 499–504 (2001).
 - 27) Blankenberg F.G. et al.: In vivo detection and imaging of phosphatidylserine expression during programmed cell death. *Proc Natl Acad Sci* **95**, 6349–6354 (1998).
 - 28) Belhocine T. et al.: In vivo imaging of chemotherapy-induced apoptosis in human cancers. *Ann NY Acad Sci* **1010**, 525–529 (2003).
 - 29) Sisson J.C. et al.: Scintigraphic localization of pheochromocytoma. *N Eng J Med* **305**, 12–17 (1981).
 - 30) Bakker W.H. et al.: [¹¹¹In-DTPA-D-Phe¹]-octreotide a potential radiopharmaceutical for imaging of somatostatin receptor-positive tumors: synthesis radiolabeling and in vitro validation. *Life Sci* **49**, 1583–1591 (1991).
 - 31) Kiesewetter D.O. et al.: Preparation of fluorine-18-labeled estrogens and their selective uptakes in target tissues of immature rats. *J Nucl Med* **25**, 1212–1221 (1984).
 - 32) Mintun M.A. et al.: Breast cancer: PET imaging of estrogen receptors. *Radiology* **169**, 45–48 (1988).
 - 33) Mankoff D.A. et al.: Characterizing tumors using metabolic imaging: PET imaging of cellular proliferation and steroid receptors. *Neoplasia* **2**, 71–88 (2000).
 - 34) Dehdashti D. et al.: Positron emission tomo-

graphic assessment of “metabolic flare” to predict response of metastatic breast cancer to antiestrogen therapy. *Eur J Nucl Med* **26**, 51–56 (1999).

35) Kao C.H. et al.: P-Glycoprotein and multidrug resistance-related protein expressions in rela-

tion to technetium-99m methoxyisobutylisonitrite scintimammography findings. *Cancer Res* **61**, 1412–1414 (2001).

36) Fuster D. et al.: Tetrofosmin as predictors of tumour response. *Q J Nucl Med* **47**, 58–62 (2003).

PROFILE



Hideshi HATTORI

Nihon Medi-Physics Co., Ltd.
Corporate Planning and Coordination Office
Strategic Marketing



Jun TOYOHARA

Nihon Medi-Physics Co., Ltd.
Research and Development Division
Research Center
Ph. D.